Available online at www.sciencedirect.com
SCIENCE DIRECT
Journal of Colloid and Interface Science 296 (2006) 150–158
JOURNAL OF Colloid and Interface Science
www.elsevier.com/locate/jcis

Electrical double layer interactions between dissimilar oxide surfaces with charge regulation and Stern–Grahame layers

Derek Y.C. Chan [a,*], Thomas W. Healy [b], Tharatorn Supasiti [a], S. Usui [c]

[a] *Department of Mathematics and Statistics, The University of Melbourne, Victoria 3010, Australia*
[b] *Department of Chemical and Biomolecular Engineering, Particulate Fluids Processing Centre, The University of Melbourne, Victoria 3010, Australia*
[c] *Tohoku University, Katahira, Aoba-ku, Sendai 980-8577, Japan*

Received 16 June 2005; accepted 1 September 2005

Available online 4 October 2005

Abstract

Models of surfaces with intrinsic ionisable amphoteric surface sites governed by the dissociation of acid–base potential determining ion species together with the capacity for the adsorption of anion and cations of the supporting electrolyte are required to describe both the results of electrokinetic and titration measurements of inorganic oxides. The Gouy–Chapman–Stern–Grahame (CGSG) model is one such model that has been widely used in the literature. The electrical double layer interaction between two dissimilar CGSG surfaces has been studied by Usui recently [S. Usui, J. Colloid Interface Sci. 280 (2004) 113] where erroneous discontinuities in the slope of the pressure–separation relation were observed. We revisit this calculation and provide a simple general methodology to analyse the electrical double layer interaction between dissimilar ionisable surfaces with ion adsorption.

Keywords: Double layer interaction; Dissimilar double layer; Charge regulation; Gouy–Chapman–Stern–Grahame model; Oxide–water interfaces; Site-binding model; Surface force

1. Introduction

The Gouy–Chapman–Stern–Grahame (CGSG) or site-binding model [1] has been used successfully to model and reconcile electrokinetic surface potential measurements of inorganic oxides with surface charge data derived from titration experiments. In this model, intrinsic amphoteric ionisable groups of the oxide surface develop a net charge in response to the solution concentration of potential determining ions or pH. In addition, the model also allows for the specific adsorption of anions and cations of the supporting electrolyte at the Stern plane. It is through the combined recognition of the ionisation of intrinsic surface groups and of ion binding in the CGSG model that made it possible to model both electrokinetic and titration data [2]. On the other hand, the CGSG model for oxides had not be been used extensively to model the electrical double layer interaction between oxide surfaces. As the state of charge of such surfaces depends on the adsorption and desorption of both potential determining ions and supporting electrolyte ions, neither the surface charge nor the surface potential are kept constant during interaction. Such surfaces are referred to as charge regulating surfaces.

Some time ago, the electrical double layer interaction between regulating amphoteric surfaces, where there is no adsorption of supporting electrolyte ions, was analysed in detail for both identical [3] and non-identical surfaces [4] using the Poisson–Boltzmann (PB) model. Numerical results for the interaction between non-identical surfaces held at different combinations of constant surface charges or surface potentials were given in [5] which generalised the earlier work that focused on the interaction between dissimilar surfaces held at constant surface potential or constant surface charge [6]. More recently, interactions between dissimilar surfaces bearing a single type of ionisable groups [7] as well as more general surface ionisations reactions [8] have been studied. Within the PB model, the interaction between flat surfaces can be obtained without having to

* Corresponding author.
E-mail address: d.chan@unimelb.edu.au (D.Y.C. Chan).

0021-9797/$ – see front matter
doi:10.1016/j.jcis.2005.09.003

solve explicitly for the potential distribution in the electrolyte between the surfaces.

Recently, Usui [9] used the CGSG model to re-examine the electrical double layer interaction between two surfaces that have like signs but different potentials at infinite separation. The model was designed to model oxide surfaces with amphoteric. This study produced results that contained unexpected abrupt changes in slope in the pressure versus separation curves. This work suggested that previous results obtained with the Gouy–Chapman model [9] where the force of interaction can change from repulsion to attraction at some particular separation were not observed using the CGSG model of the double layer.

In this paper, we revisit the CGSG model for the electrical double layer interaction between two like charged surfaces which have potentials of the same sign but different in magnitude when they are at infinite separation. We follow the formalism developed earlier [4,5] to develop a general approach to analyse the double layer interactions under the CGSG model. We will show that the earlier calculation [9] was incorrect in suggesting that there were discontinuities in the slope of the variations of the pressure with separation.

2. Formulation

2.1. Surface potentials and charges

A schematic of the Gouy–Chapman–Stern–Grahame (CGSG) model is depicted in Fig. 1 and the we recall the main features of this model [1]. The interacting oxide surfaces develop a surface charge as a result of the dissociation of proton from amphoteric surface groups:

$$\mathrm{AH_2^+} \Leftrightarrow \mathrm{AH} + \mathrm{H^+}, \qquad \mathrm{AH} \Leftrightarrow \mathrm{A^-} + \mathrm{H^+}. \tag{1}$$

These reactions are characterised by dissociation constants K_+ and K_- according to the mass action equations

$$\frac{[\mathrm{AH}]H\exp(-e\psi_\mathrm{o}/kT)}{[\mathrm{AH_2^+}]} = K_+,$$
$$\frac{[\mathrm{A^-}]H\exp(-e\psi_\mathrm{o}/kT)}{[\mathrm{AH}]} = K_-, \tag{2}$$

where H is the bulk concentration of $\mathrm{H^+}$ ions and ψ_o is the potential at the oxide surface. In the CGSG model, similar surface complexation reactions are assumed to occur in the Stern plane for cations and anions that make up the univalent electrolyte:

$$\mathrm{AH_2^+X^-} \Leftrightarrow \mathrm{AH_2^+} + \mathrm{X^-}, \qquad \mathrm{A^-M^+} \Leftrightarrow \mathrm{A^-} + \mathrm{M^+}. \tag{3}$$

These reactions are characterised by dissociation constants K_A and K_C for the anions and cations,

$$\frac{[\mathrm{AH_2^+}]c\exp(+e\psi_\beta/kT)}{[\mathrm{AH_2^+X^-}]} = K_\mathrm{A},$$
$$\frac{[\mathrm{A^-}]c\exp(-e\psi_\beta/kT)}{[\mathrm{A^-M^+}]} = K_\mathrm{C}, \tag{4}$$

with c being the bulk (molar) concentration of univalent electrolyte $\mathrm{M^+X^-}$. The potential at the Stern plane is denoted by ψ_β (see Fig. 1).

With N_s ionisable sites per unit area of the oxide surface, the surface charge density on the oxide surface is (e is the protonic charge)

$$\sigma_\mathrm{o} = eN_\mathrm{s}\frac{[\mathrm{AH_2^+}] - [\mathrm{A^-}] + [\mathrm{AH_2^+X^-}] - [\mathrm{A^-M^+}]}{[\mathrm{AH}] + [\mathrm{AH_2^+}] + [\mathrm{A^-}] + [\mathrm{A^-M^+}] + [\mathrm{AH_2^+X^-}]}$$
$$\equiv eN_\mathrm{s}\alpha_\mathrm{o}, \tag{5}$$

and the surface charge density in the Stern layer, due to bound ions and assuming the same number of ionisable sites as at the oxide surface, is

$$\sigma_\beta = eN_\mathrm{s}\frac{[\mathrm{A^-M^+}] - [\mathrm{AH_2^+X^-}]}{[\mathrm{AH}] + [\mathrm{AH_2^+}] + [\mathrm{A^-}] + [\mathrm{A^-M^+}] + [\mathrm{AH_2^+X}]}$$
$$\equiv eN_\mathrm{s}\alpha_\beta. \tag{6}$$

The degree of ionisation at the oxide surface α_o and at the Stern plane α_β is defined by these equations with $-1 < \alpha_\mathrm{o}, \alpha_\beta < 1$.

In the CGSG model, the relations between the potential at the oxide surface ψ_o, the potential at the Stern plane ψ_β, and the potential at the boundary of the diffuse double layer ψ_d, are related to the surface charges by the capacitances (per unit area) of the inner layer K_i and outer layer K_o of the Stern region (see

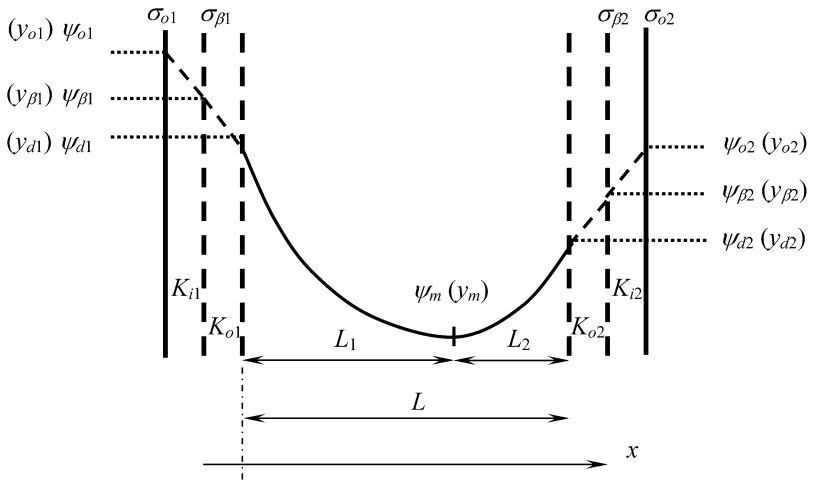

Fig. 1. Schematic diagram of the Gouy–Chapman–Stern–Grahame model of interacting oxide surfaces.

Fig. 1). These relationships are

$$\sigma_o = K_i(\psi_o - \psi_\beta), \tag{7a}$$

$$\sigma_\beta = -K_i(\psi_o - \psi_\beta) + K_o(\psi_\beta - \psi_d). \tag{7b}$$

2.2. Interacting diffuse double layer

Outside the Stern layer, the potential in the diffuse double layer is given by the Poisson–Boltzmann (PB) model (see Fig. 1). In terms of the scaled potential $y(x) = e\psi(x)/kT$, the PB equation reads $d^2y/dx^2 = \kappa^2 \sinh y$, where $\kappa = (2ne^2/\varepsilon_o\varepsilon_r kT)^{1/2}$ is the reciprocal of the Debye length and $n = (1000cN_A)$ is the number concentration of the electrolyte. We consider the case in which the potentials on each surface have the same sign and we can without loss of generality assume that the sign is positive. It is well known that solution of the PB equation in this case has two different forms:

(a) If a potential minimum y_m (see Fig. 1) *exists* between the two surfaces, the interaction is always repulsive and the separation L is related to the force per unit area or pressure $P \equiv 2nkTp$ by

$$\begin{aligned}\kappa L &= \kappa L_1 + \kappa L_2 \\ &= \int_{y_m}^{y_{d1}} \frac{dy}{\sqrt{2(\cosh y - p - 1)}} + \int_{y_m}^{y_{d2}} \frac{dy}{\sqrt{2(\cosh y - p - 1)}} \\ &= 2\exp(-y_m/2)\big[F(\pi/2, m) - F(\phi_1, m) - F(\phi_2, m)\big],\end{aligned} \tag{8}$$

where $F(\phi, m) \equiv \int_0^\phi d\theta/\sqrt{1 - m\sin^2\theta}$ is the elliptic integral of the first kind [10], with $m \equiv \exp(-2y_m)$ and $\phi_i \equiv \arcsin(\exp[-(y_{di} - y_m)/2])$, $i = 1, 2$. In this case, the scaled surface is related to the potential minimum y_m by $p = (\cosh y_m - 1) > 0$. It is useful to express the integrals in terms of elliptic integrals as in Eq. (8) since the integrands have integrable singularities at the lower limit $y = y_m$.

(b) If a potential minimum *does not exist* between the two surfaces, the interaction may be repulsive ($p > 0$) or attractive ($p < 0$) and the separation L is related to the scaled pressure p by

$$\kappa L = \int_{y_{d2}}^{y_{d1}} \frac{dy}{\sqrt{2(\cosh y - p - 1)}}. \tag{9}$$

This integral can be evaluated numerically since the integrand is finite over the range of integration. This result applies even in the case where y_{d1} and y_{d2} have opposite signs.

For a given value of the scaled pressure p, the graphical analysis described below will help determine whether Eq. (8) or (9) is the appropriate equation to use to calculate the separation L.

Finally, the relationship between the scaled pressure p and scaled diffuse layer potentials y_{d1} and y_{d2} follows from the electroneutrality or Gaussian electrostatic boundary conditions

$$\begin{aligned}&x = 0: \\ &-\varepsilon_o\varepsilon_r\frac{d\psi}{dx} = \sigma_{o1} + \sigma_{\beta 1} \\ &\qquad = (\kappa\varepsilon_o\varepsilon_r kT/e)\big[4\sinh^2(y_{d1}/2) - 2p\big]^{1/2} \\ &\qquad \equiv -\sigma_{d1},\end{aligned} \tag{10}$$

$$\begin{aligned}&x = L: \\ &\varepsilon_o\varepsilon_r\frac{d\psi}{dx} = \sigma_{o2} + \sigma_{\beta 2} \\ &\qquad = -(\kappa\varepsilon_o\varepsilon_r kT/e)\big[4\sinh^2(y_{d2}/2) - 2p\big]^{1/2} \\ &\qquad \equiv -\sigma_{d2},\end{aligned} \tag{11}$$

where σ_d is referred to as the diffuse layer charge.

2.3. Analysis and method of solution

While the electrical double layer interaction in the CGSG model can be obtained by solving Eqs. (1)–(11), a practical implementation requires choosing the appropriate variables to use in a numerical scheme. In general terms, Eqs. (10) and (11) relate the scaled pressure p to the scaled diffuse layer potentials y_{d1} and y_{d2}, and the separation can then be obtained from either Eq. (8) or (9). Specifically we will delineate the steps required to solve Eqs. (10) and (11) for an appropriate value of the scaled pressure p and then choose either Eq. (8) or (9) as required to calculate the separation corresponding to the scaled pressure.

Using Eqs. (2) and (4), the expressions for the degree of ionisation α_o and α_β can be written in terms of the scaled potential y_o using Eqs. (2), (4) and (7):

$$\alpha_o = \frac{\delta_o \sinh(y_N - y_o)\delta_\beta \sinh(\gamma\alpha_o - \eta)}{1 + \delta_o\cosh(y_N - y_o) + \delta_\beta\cosh(\gamma\alpha_o - \eta)}, \tag{12}$$

$$\alpha_\beta = \frac{\delta_\beta \sinh(\gamma_o\alpha_o - \eta_o)}{1 + \delta_o\cosh(y_N - y_o) + \delta_\beta\cosh(\gamma\alpha_o - \eta)}. \tag{13}$$

The various constants in Eqs. (12) and (13) are given by

$$\begin{aligned}&\Delta pK = pK_- - pK_+, \\ &\delta_o = 2(K_-/K_+)^{1/2} = 2\times 10^{-\Delta pK/2}, \\ &\delta_\beta = 2c\left(\frac{K_-}{K_+K_AK_C}\right)^{1/2}, \\ &pH_o = \frac{1}{2}(pK_+ + pK_-), \\ &\Delta pH = pH_o - pH, \\ &y_N = \ln(10)\Delta pH, \qquad \gamma = \frac{e^2N_s}{kTK_i}, \\ &\eta = \ln(10)\left[\frac{1}{2}(pK_A - pK_C) + pH_o - pH\right].\end{aligned} \tag{14}$$

These dimensionless constants in (14) depend on the intrinsic properties of the ionisable surfaces, the various dissociation constants and the ionic composition of solution. In deriving Eq. (12), we have used Eq. (7a) to eliminate y_β in favour of y_o to obtain an implicit equation for α_o in terms of y_o which is straightforward to solve numerically. Once α_o and y_o are known, α_β can be calculated from Eq. (13). Then using

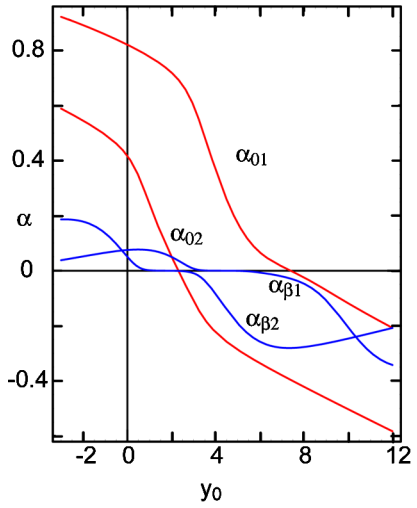

Fig. 2. The degree of dissociation at the oxide surface α_o and at the Stern plane α_β of each surface as functions of the potential y_o for data in Tables 1 and 2 at pH 6 and electrolyte concentration $c = 1$ mM.

Eq. (7b), the diffuse double layer potentials y_{d1} and y_{d2} at each surface can be related to y_o by the corresponding equation at each surface:

$$y_d = y_o - \gamma\left\{\alpha_o + \frac{K_i}{K_o}(\alpha_o + \alpha_\beta)\right\}. \tag{15}$$

In Fig. 2, we show the variation of the degree of dissociation α_o and α_β in terms of y_o for system parameters given in Tables 1 and 2. These results are obtained by the solution procedure described above.

In order to visualise qualitatively the variations of the pressure with separation we generalise the method developed previously for analysing the double layer interaction between dissimilar surfaces [4,5]. We plot the square of the total surface charge density $\sigma^2 = (\sigma_o + \sigma_\beta)^2$ for each surface as functions of y_d (Fig. 3). At any separation, the total charge σ and the diffuse layer scaled potential y_d of each surface must lie on the corresponding $\sigma^2(y_d)$ curve. Thus the $\sigma^2(y_d)$ curve may be regarded as the equation of state for each surface.

Table 1
Parameters for both model oxide surfaces

N_s (sites/cm^{-2})	K_A (M)	K_C (M)	K_i (μF/cm^{-2})	K_o (μF/cm^{-2})
5×10^{14}	1	1	140	20

Table 2
Values for ΔpK and pH_o of the model oxide surfaces (the solution pH = 6 and the electrolyte concentration is $c = 1$ mM)

Surface	ΔpK	pH_o
1	3	9
2	2	7

Also plotted in Fig. 3 is the function $s(y_d) \equiv (2\kappa\varepsilon_o\varepsilon_r \times kT/e)^2 \sinh^2(y_d/2)$. From Eqs. (10) and (11), we see that the vertical distance between $s(y_d)$ and each charge density curve for σ^2 is proportional to the scaled pressure p. The pressure on each surface must, of course, be the same. As the separation between the surfaces changes, each surface must travel along its own σ^2 curve but the position along each σ^2 curve must maintain the same vertical distance from the curve $s(y_d)$ since this distance is proportional to the pressure between the surfaces.

At infinite separation where the pressure on each plate is zero, each surface will be located at y_{d1}^∞ and y_{d2}^∞, respectively, where the σ^2 curves intersect the $s(y_d)$ curve. As the separation decreases, the scaled potential y_{d2} of surface 2 (surface 2 is designated as the surface with the lower y_d^∞) will increase monotonically along σ_2^2 and correspondingly y_{d1} will move along σ_1^2 while maintaining the same vertical distance from the curve $s(y_d)$ as y_{d2}. This will continue until both surfaces reach the point y_d^* at zero separation $L = 0$, when both surfaces will attain the same scaled diffuse layer potential: $y_{d1} = y_d^* = y_{d2}$.

Between y_{d2}^∞ and y_{d2}^0 (where $\sigma_2 = 0$), $\sigma_2 = (\sigma_{o2} + \sigma_{\beta 2})$ is positive and has the same sign as σ_1, so a potential minimum will exist between the surfaces and thus Eq. (8) should be used

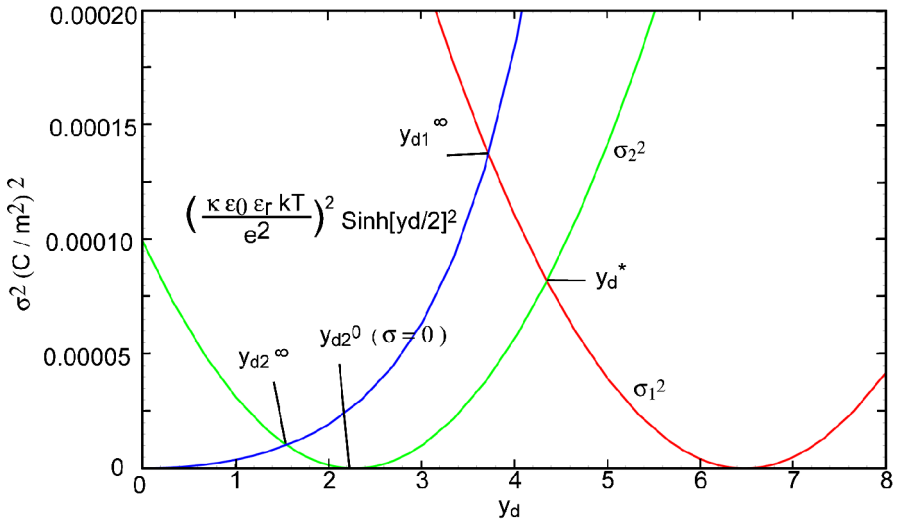

Fig. 3. The square of the total charge for each surface $\sigma^2 = (\sigma_o + \sigma_\beta)^2$ as functions of the potential y_d. Superimposed is the curve for $(2\kappa\varepsilon_o\varepsilon_r kT/e)^2 \sinh^2(y_d/2)$ for data in Tables 1 and 2 at pH 6 and electrolyte concentration $c = 1$ mM.

to calculate the separation. Between y_{d2}^{0} and y_{d}^{*}, σ_2 is negative and has the opposite sign to σ_1, so a potential minimum will not exist between the surfaces and thus Eq. (9) should therefore be used to calculate the separation. During the course of the interaction, the total charge of the surface with the lower y_{d}^{∞} (which we have designated as surface 2) will always change sign.

This method of visualising the evolution of the diffuse layer potential y_d and the total surface charge density $\sigma = (\sigma_o + \sigma_\beta)$ of each surface provides a simple and systematic way to track and compute the relationship between the separation L and the scaled pressure p using either Eq. (8) or (9) as appropriate. Thus by using the scaled potential y_{d2} as the parametric variable and by stepping monotonically from y_{d2}^{∞} to y_{d}^{*} we can compute the pressure and the corresponding separation at each step.

3. Results and discussion

We provide numerical results to illustrate the behaviour of the CGSG model using parameters given in Tables 1 and 2 at a solution pH = 6 and 1:1 electrolyte concentration $c = 1$ mM. These are representative data for inorganic oxide systems.

3.1. Pressure

As an illustration of the differences between the double layer interaction in the CGSG model, constant potential and constant charge, we compare the variation of the pressure for these three cases as functions of separation in Fig. 4. For this set of input parameters, the pressure predicted by the CGSG as well as the constant surface charge model is monotonic and repulsive for all separations. For this case of non-identical surfaces with like signs, the pressure for the constant potential model is repulsive for large separation but becomes attractive at small separations. The constant potential model corresponds to perfect regulation. As expected, the CGSG pressure lies between the constant potential and constant models.

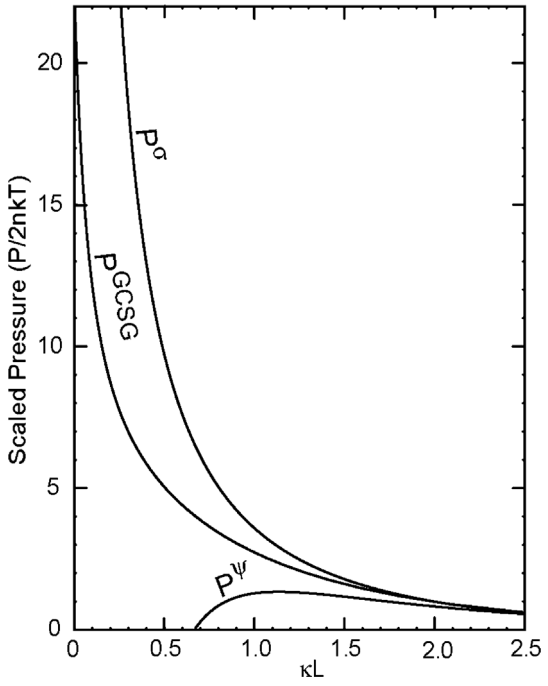

Fig. 4. The pressure as a function of the separation for data in Tables 1 and 2 at pH 6 and electrolyte concentration $c = 1$ mM. Corresponding results for interaction at constant surface potential P^{ψ} and at constant surface charge P^{σ}, all with the same diffuse layer potentials y_{d1}^{∞} and y_{d2}^{∞} at infinite separation, are given for comparison.

3.2. Surface potentials

In Fig. 5 we show variations of the scaled potentials at the oxide surface y_o, at the Stern plane y_β and at the diffuse layer y_d at each surface as functions of the separation. The potentials y_{o1}, $y_{\beta 1}$ and y_{d1} at surface 1, the surface with the higher diffuse layer potential y_d at infinite separation, are quite featureless. The percentage variation of these potentials is small for all separations and it behaves almost like a constant potential surface.

On the other hand, there are a number of interesting features in the variations of the potentials on the surface 2, the surface with the lower diffuse layer potential y_d at infinite separation. At large separations, the relative magnitudes of the three potentials are $y_{o2} > y_{\beta 2} > y_{d2}$. As the separation decreases, the diffuse layer potential y_{d2} increases rapidly and at κL between 0.5 to 0.7, the order of the relative magnitudes reverses to $y_{o2} < y_{\beta 2} < y_{d2}$ so that at small separation, y_{d2} changes

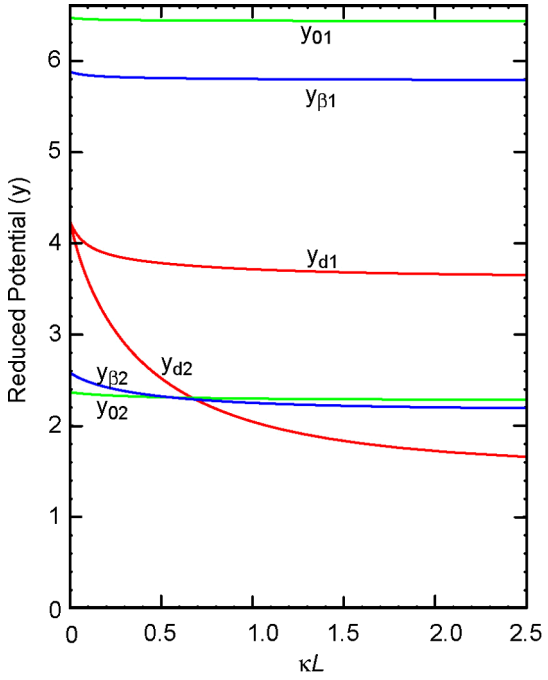

Fig. 5. Variations of the scaled potentials at the oxide surface y_o, at the Stern plane y_β and at the diffuse layer y_d at each surface as functions of the separation for data in Tables 1 and 2 at pH 6 and electrolyte concentration $c = 1$ mM.

from the lowest to the highest of the three potentials on surface 2. As the separation L approaches 0, we note as expected that the diffuse layer potential of both surfaces becomes equal: $y_{d1} = y_{d}^{*} = y_{d2}$.

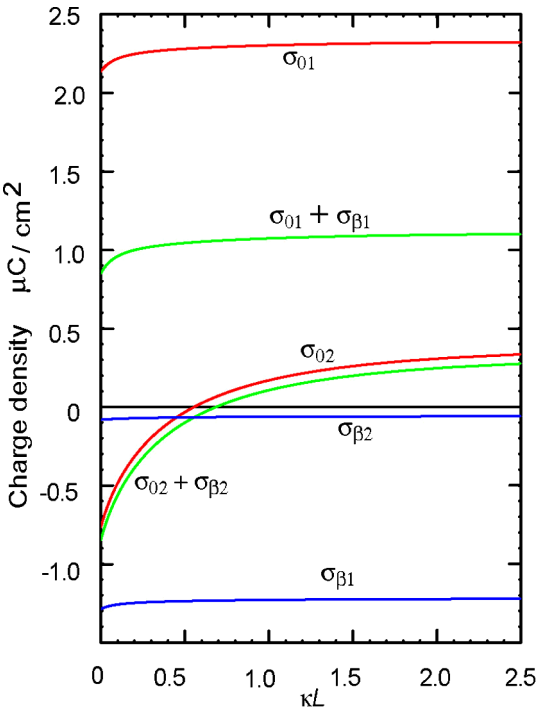

Fig. 6. Variations of the surface charge density at the oxide surface σ_o, at the Stern plane σ_β and the total charge density $\sigma = \sigma_o + \sigma_\beta$ at each surface as functions of the separation for data in Tables 1 and 2 at pH 6 and electrolyte concentration $c = 1$ mM.

3.3. Surface charge densities

The behaviour of the surface potentials with separation is mirrored by the variations in the surface charge at the oxide surface σ_o and at the Stern plane σ_β (see Fig. 6). The charge density that varies the most with separation is the charge σ_{o2} at the oxide surface of surface 2 which changes sign at $\kappa L \sim 0.7$. Hence it is the change in ionisation of the surface groups at the oxide surface with the lower diffuse layer potential at infinite separation that is mainly responsible for the variation of the potentials seen in Fig. 5.

3.4. Ion concentrations at the Stern plane

To illustrate variations in the anions and cations concentration at the Stern plane during interaction, we plot the ratio of the ion concentration at the Stern plane relative to the bulk concentration at each surface in Fig. 7. We observe that the changes in the concentration of ions at the Stern plane on surface 1 (the surface with the higher diffuse layer potential at infinite separation) are relatively small with variations in separation. This is consistent with the earlier observation that the potentials on surface 1 hardly vary. On the other hand, variations in the concentration of anions and cations at the Stern plane of surface are of the order 30 to 50% of the bulk value.

3.5. Different surface properties

We can obtain interesting non-monotonic behaviour in the pressure and surface potential by changing the properties of surface 2, the surface with the lower surface potential at infinite separation. To illustrate this, we use $pH_{o2} = 6.55$ for surface 2 instead of $pH_{o2} = 7$ (Table 2), while keeping all other surface parameters the same as before including a solution $pH = 6$ and $c = 1$ mM of 1:1 electrolyte. With this change, the pressure is no longer a monotonic function of separation (see Fig. 8). This behaviour is a consequence of the variations in relative curvature between the function $s(y_d) \equiv (2\kappa\varepsilon_o\varepsilon_r kT/e)^2 \sinh^2(y_d/2)$ and the total charge curve $\sigma_2^2(y_d)$ of surface 2 because the variation of the pressure with separation is determined by the vertical distance between these two curves (see Fig. 9). In Fig. 10, we see that the non-monotonic behaviour of the pressure with separation is also mirrored in the variations of the surface potential at surface 1, the surface with the higher diffuse layer potential at infinite separation. Similarly, the density of ions at the Stern plane of surface 1 is also a non-monotonic function of separation, Fig. 11. The potential and charge on surface 2 remain monotonic with variations in separation (not shown). However, in both cases such variations are small in relative terms.

In Fig. 12 we demonstrate possible characteristics of the pressure upon changing the isoelectric points of the surface

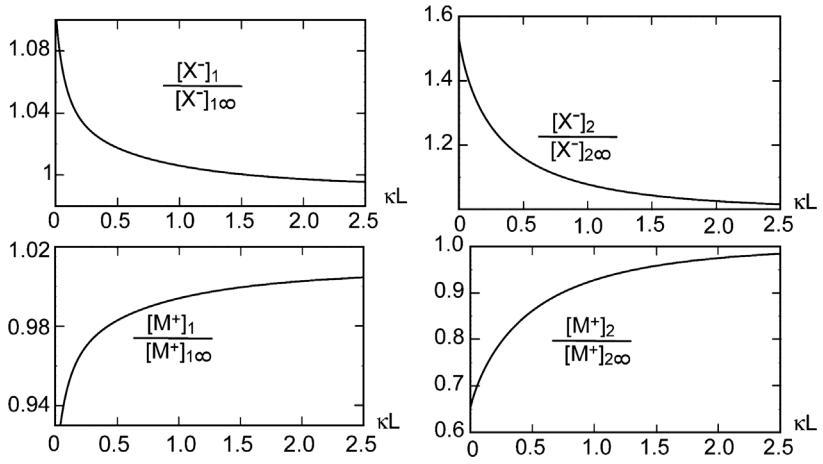

Fig. 7. Variations of ratio of cation and anion concentrations at the Stern plane of each surface relative to the corresponding bulk concentrations as functions of the separation for data in Tables 1 and 2 at pH 6 and electrolyte concentration $c = 1$ mM.

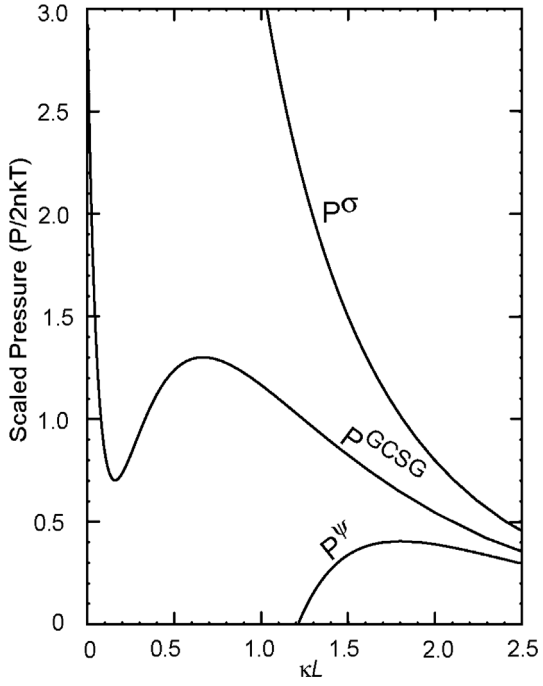

Fig. 8. The pressure as a function of the separation at pH 6 and electrolyte concentration $c = 1$ mM for data in Tables 1 and 2 except $\mathrm{pH}_{o2} = 6.55$. Corresponding results for interaction at constant surface potential P^{ψ} and at constant surface charge P^{σ}, all with the same diffuse layer potentials y_{d1}^{∞} and y_{d2}^{∞} at infinite separation, are given for comparison.

with the lower surface potential at infinite separation (surface 2) whose surface properties are key in determining the form of the pressure vs separation curve. Take, for instance, two surfaces with isoelectric points: $\mathrm{pH}_{o2} = 6.50$ and $\mathrm{pH}_{o2} = 6.55$. The double layer interaction takes place under the same solution pH = 6, electrolyte concentration $c = 1$ mM and other system parameters as given in Tables 1 and 2. As a result of subtle differences in the curvatures in the charge curve of the surface with the lower surface potential at infinite separation (surface 2) and the diffuse layer charge curve $s(y_d) \equiv (2\kappa\varepsilon_o\varepsilon_r kT/e)^2 \sinh^2(y_d/2)$ (see Fig. 9), this slight change in the isoelectric point can result in the pressure having a negative region that corresponds to an attraction at small separations. The observed non-monotonic variation of the pressure with separation can also be brought about by increasing the solution pH by about 0.5 units while keeping the isoelectric point of surface 2 constant at $\mathrm{pH}_{o2} = 6.0$. The reason for this is that this increase in solution pH also has the effect of bringing the charge curve of the surface 2 and the diffuse layer charge curve $s(y_d)$ closer together.

The key observation is that the general behaviour of the variation of the pressure with separation is controlled by the characteristic curvature and the relative position of the charge curve of surface 2, the surface with the lower surface potential at infinite separation relative to the diffuse layer charge curve $s(y_d)$. The precise magnitude of the pressure variations can obviously be affected by changing the adsorption characteristics of the supporting electrolyte M^+X^- and the pK values of the amphoteric ionisable groups on surface 2; however, such effects are less important provided the isoelectric points of the two interacting surfaces are more than about 2 pH units apart.

Finally, in Fig. 13 we compare the variations of the interaction energy per unit area obtained by integrating the pressure with respect to separation for $\mathrm{pH}_{o2} = 6.5$, 6.55 and 7. The maximum and minimum in the pressure in Fig. 8 for $\mathrm{pH}_{o2} = 6.55$ give rise to an inflection in the energy curve.

More generally, the appearance of van der Waals loops in the pressure as shown in Fig. 12 suggests the possibility of a phase equilibrium or phase separation when such dissimilar plates are stacked in an alternating lamella configuration.

4. Summary

In this paper, we outlined a simple procedure to analyse the behaviour of the electrical double interaction between similarly charged oxide surfaces described by the Gouy–Chapman–Stern–Grahame model. Numerical results for variations of the

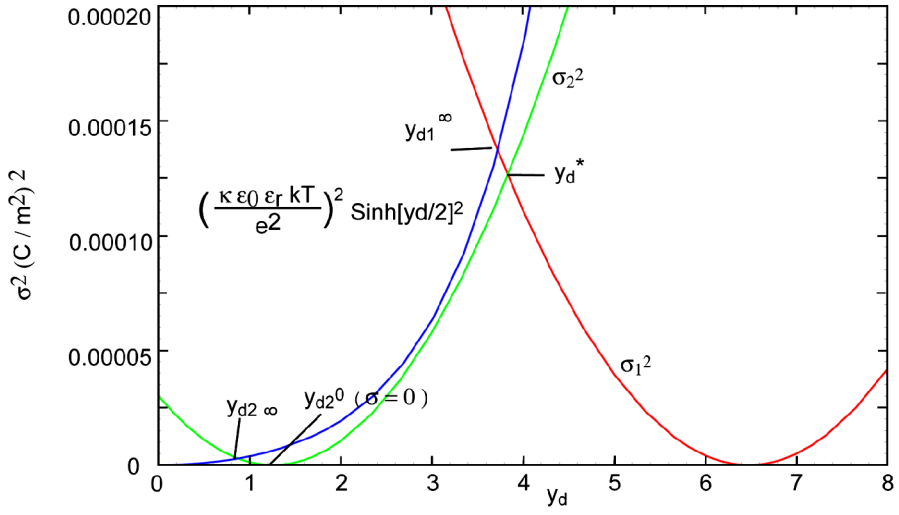

Fig. 9. The square of the total charge of each surface $\sigma^2 = (\sigma_o + \sigma_\beta)^2$ as functions of the potential y_d. Superimposed is the curve for $(2\kappa\varepsilon_o\varepsilon_r kT/e)^2 \sinh^2(y_d/2)$ at pH 6 and electrolyte concentration $c = 1$ mM, for data in Tables 1 and 2 except $\mathrm{pH}_{o2} = 6.55$.

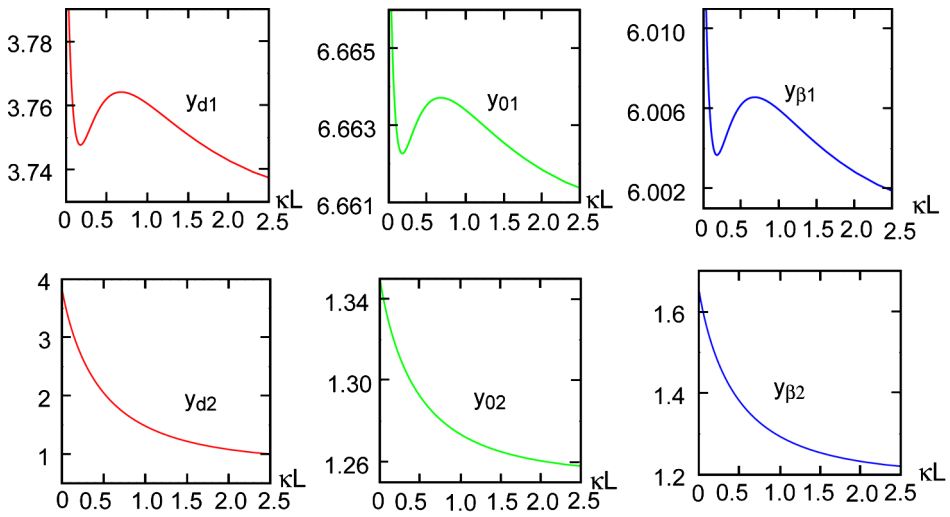

Fig. 10. Variations of the scaled potentials at the oxide surface y_o, at the Stern plane y_β and at the diffuse layer y_d at each surface as functions of the separation for data in Tables 1 and 2, except $pH_{o2} = 6.55$, at pH 6 and electrolyte concentration $c = 1$ mM.

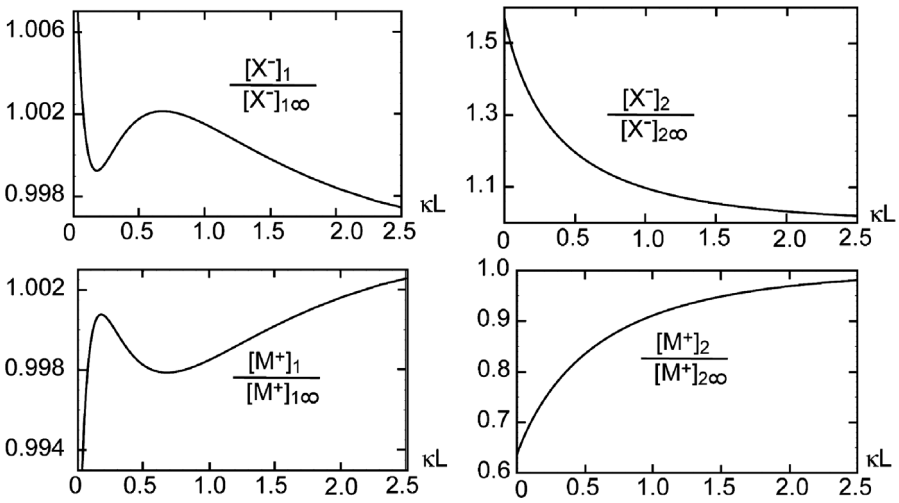

Fig. 11. Variations of ratio of cation and anion concentrations at the Stern plane of each surface relative to the corresponding bulk concentrations as functions of the separation at pH 6, electrolyte concentration $c = 1$ mM and for data in Tables 1 and 2, except $pH_{o2} = 6.55$.

pressure, surface potentials at the oxide surface and at the Stern plane, as well as ion densities at these two planes, are given. This model gives rise to non-monotonic behaviour of the pressure which can be tested by direct force measurements. There may be implications of this non-monotonic behaviour arising from dissimilar double layer interactions in the context of particle capture in bubble flotation phenomena.

More generally, we presented a method outlined in Section 2.3 to extract qualitative features of the pressure–separation curves. This method is an extension of the method used to analyse the simpler Gouy–Chapman model [4]. In particular, features such as the existence of maxima, minima or sign changes in the pressure–separation behaviour can be deduced from a plot of the variation of the square total surface charge density on each surface with the diffuse layer potential (see Fig. 3). Such a diagram can also be used to predict and track the qualitative variations of the diffuse layer potentials and the variations of the total surface charge densities on each surface. This method of analysis can readily be extended to consider interaction between surfaces of opposite signs under the CGSG models or other generalisations of the regulation model.

The method employed in this paper to calculate the relation between the pressure and the separation by using either Eq. (8) or (9) is simpler than earlier method [5] that involved the consideration of multiple cases and the needs to compute elliptic functions. This simplicity also avoid the possibility of invalid results [9].

Acknowledgments

This work is supported in part by the Particulate Fluids Processing Centre, a Special Research Centre of the Australian Research Council, and forms part of a long standing and ongoing collaboration between Tohoku University and the University of Melbourne.

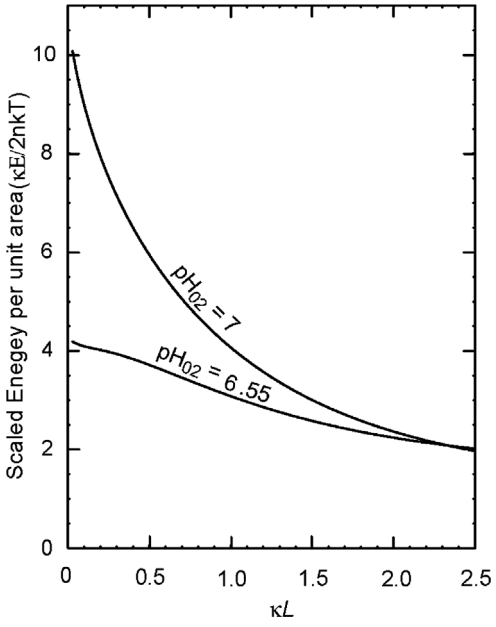

Fig. 12. A comparison of the pressure as a function of the separation at pH 6 and electrolyte concentration $c = 1$ mM for data in Tables 1 and 2 for two different values of the isoelectric point of surface 2: $pH_{o2} = 6.5$ and $pH_{o2} = 6.55$.

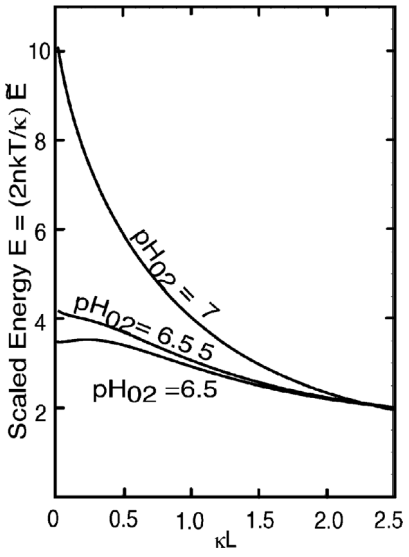

Fig. 13. The interaction free energy per unit area scaled by $(2nkT/\kappa)$ as a function of the separation at pH 6 and electrolyte concentration $c = 1$ mM for $pH_{o2} = 6.5$, 6.55 and 7. Other data are given in Tables 1 and 2.

References

[1] D.E. Yates, S. Levine, T.W. Healy, J. Chem. Soc. Faraday I 70 (1974) 1807.
[2] D.E. Yates, T.W. Healy, J. Colloid Interface Sci. 55 (1976) 9.
[3] D.Y.C. Chan, T.W. Healy, J.W. Perram, L.R. White, J. Chem. Soc. Faraday I 71 (1975) 1046.
[4] D.Y.C. Chan, T.W. Healy, L.R. White, J. Chem. Soc. Faraday I 76 (1977) 2844.
[5] D. MacCormack, S.L. Carnie, D.Y.C. Chan, J. Colloid Interface Sci. 169 (1995) 177.
[6] B.V. Deryaguin, Discuss Faraday Soc. 18 (1954) 85;
O.F. Devereux, P.L. de Bruyn, Interaction of Plane Parallel Double Layers, MIT Press, Cambridge, 1963;
G.M. Bell, G.C. Peterson, J. Colloid Interface Sci. 41 (1972) 542;
V.A. Parsegian, D. Gingell, Biophys. J. 12 (1972) 1192.
[7] S.H. Behrens, M. Borkevec, Phys. Rev. E 60 (1999) 7040;
P.M. Biesheuvel, J. Colloid Interface Sci. 275 (2004) 514.
[8] Yu.V. Shulepov, L.L. Koopal, J. Lyklema, S.S. Dhkhin, Colloids Surf. A 131 (1998) 51;
J. Lyklema, J.F.L. Duval, Adv. Colloid Interface Sci. 114–115 (2005) 27.
[9] S. Usui, J. Colloid Interface Sci. 280 (2004) 113.
[10] M. Abramowich, I.A. Stegun, Handbook of Mathematical Functions, National Bureau of Standards, 1964.